HEAT TRANSFER ENHANCEMENT IN SMOOTH AND CORRUGATED MICROCHANNELS

Fernando V. Castellões[1] and Renato M. Cotta
Laboratory of Transmission and Technology of Heat - LTTC
Mechanical Engineering Dept.- EE-COPPE/UFRJ
Universidade Federal do Rio de Janeiro, Cx. Postal 68503 - Rio de Janeiro, RJ, 21945-970, Brasil
[1]Petrobras R&D Center – CENPES, Rio de Janeiro, RJ, Brasil

Abstract

The present lecture reports the analysis of combining micro-channels with wall corrugation as a thermal exchange intensification mechanism aimed at new applications in high performance cooling. The proposed model involves axial heat diffusion along the fluid and adiabatic regions both upstream and downstream to the corrugated heat transfer section, in light of the lower values of Reynolds numbers (and consequently Peclet numbers) that can be encountered in the present class of problems. Aimed at developing a fast and reliable methodology for optimization purposes, the related laminar velocity field is obtained by an approximate analytical solution valid for smooth corrugations and low Reynolds numbers, typical of the analyzed micro-channel configurations, locally satisfying the continuity equation. A hybrid numerical-analytical solution methodology for the energy equation is proposed, based on the Generalized Integral Transform Technique (GITT) in partial transformation mode, and for a transient formulation. The hybrid approach is first validated for the case of a smooth parallel-plates channel situation, and the importance of axial heat conduction along the fluid is then demonstrated. Heat transfer enhancement is analyzed in terms of the local Nusselt number and dimensionless bulk temperature along the heat transfer section. An illustrative sinusoidal corrugation shape is adopted and the influence of Reynolds number and corrugation geometric parameters is discussed

KEYWORDS

Micro-channels, corrugated walls, heat transfer enhancement, forced convection, integral transforms.

INTRODUCTION

Nanotechnology and micro-fabrication techniques have been allowing for the enhancement and development of a number of engineering applications, while providing new challenging scientific perspectives in fundamental research. Within the scope of thermal engineering, energy conservation and sustainable development demands have been driving research efforts towards more energy efficient equipments and processes. In this context, the scale reduction in mechanical fabrication has been permitting the miniaturization of thermal devices, such as in the case of micro-heat exchangers. Novel experimental, modeling and simulation approaches have been required to explain deviations of the heat transfer behavior of micro-systems as compared to classical macro-scale phenomena. Our research effort in this context is related to the fundamental analysis of forced convection within micro-channels, as required for the design of micro-heat exchangers, including the effects of axial heat conduction and wall corrugation or roughness on heat transfer enhancement. The present lecture is thus aimed at illustrating some of the research work undertaken at COPPE/UFRJ, jointly with CENPES, the Petrobras Research Center, in Rio de Janeiro, Brasil, towards the characterization, modeling, and simulation of micro-channels and their associated thermal convective behavior.

The petroleum and process industries have been quite active in progressively incorporating heat transfer enhancement solutions to the efficiency increase requirements along the years [1]. More recently, heat exchangers employing micro-channels with characteristic dimensions below 500 microns have been calling the attention of researchers and practitioners, towards applications that require high heat removal demands and/or space and weight limitations [2]. Motivated by the search for optimal solutions in heat exchange rates, Steinke & Kandlikar [3] critically analyzed various heat transfer enhancement techniques as applied to the micro-channels scale. Among the passive enhancement techniques then discussed, the authors emphasize the utilization of treated surfaces, rough or corrugated walls and additives for working fluids. Several other approaches were disregarded

in light of the difficulties in manufacturing or mechanically modifying the thermal system at the micro-scale. In parallel, a few previous works have addressed the interest in investigating channel corrugations at the micro-scale, either for liquid or gaseous flows [4, 5].

In this context, the research here reported addresses the convective heat transfer within micro-channels possibly enhanced by the presence of axial heat conduction and wall corrugations. First, the typical low Reynolds numbers in such micro-systems may lead to low values of the Peclet number that bring up some relevance to the axial heat diffusion along the fluid stream, especially for regions close to the inlet. Then, both the upstream and downstream sections of the micro-channel that are not actually part of the heat transfer section, may participate in the overall heat transfer process, and finally yield different predictions than those reached by making use of conventional macro-scale relations for ordinary liquids or gases. Therefore, our first objective is to inspect such effects of the axial heat diffusion within the fluid. For this reason, it was initially necessary to identify the range of governing parameters to be analyzed, in order to allow for an appropriate modeling of the relevant physical phenomena that may appear at this dimensional scale [6]. Second, either due to the inherent difficulties in achieving smooth surfaces during micro-fabrication processes or to the actual purpose of improving mixing and/or heat transfer, micro-channels with irregularly shaped walls started gaining some focus in the heat and mass transfer literature, as pointed out in the brief review above. Thus, the analysis of laminar forced convection within micro-channels with corrugated walls, and the possible heat transfer enhancement effect achieved, is another objective of the present study.

The steady two-dimensional flow problem was handled by adopting an approximate analytical solution that essentially adapts the fully developed velocity profile to the wall geometric variations, just satisfying the continuity equation [7]. Such simplified approach was introduced in [7] aimed at the solution of incompressible flow problems in low Reynolds number situations and gradual geometric variations in wall corrugations. The solution methodology for the energy equation first introduces a domain decomposition strategy, redefining the coordinates systems for the three heat transfer regions, so as to rewrite the problem in the form of a system of equations within the same mathematical domain, coupled at the interfaces of the three regions. Then, a hybrid numerical-analytical solution based on the Generalized Integral Transform Technique (GITT) is proposed [8–10], which consists on the elimination of the transversal coordinate by integral transformation, and results in a coupled system of one-dimensional partial differential equations for the transformed temperatures. This system is then handled numerically with local error control by making use of the Method of Lines implemented in the *Mathematica* 5.2 system [11]. This so-called partial transformation mode of the GITT allows for the accurate and flexible solution of multidimensional partial differential systems [12] and has been previously employed in the solution of transient and periodic forced convection within smooth parallel-plates micro-channels [13–15]. This alternative hybrid solution strategy to the more usual full integral transformation mode is of particular interest in the treatment of transient convection-diffusion problems with a preferential convective direction. In such cases, the partial integral transformation in all but one space coordinate, may offer an interesting combination of relative advantages between the eigenfunction expansion approach and the selected numerical method for handling the coupled system of one-dimensional partial differential equations that results from the transformation procedure [13].

The situation of a smooth parallel-plates channel is first analyzed, for typical values of the governing parameters, so as to provide validations of the hybrid numerical-analytical solution for the energy equation, while also illustrating the importance of the axial heat diffusion along the fluid, especially in the transition from the first adiabatic region and the heat transfer section. Then, the approximate analytical solution of the flow problem is demonstrated, as compared to benchmark results of the two dimensional Navier-Stokes equations, as obtained from the GITT itself in previous works [16, 17]. The illustrative situation of sinusoidal symmetric corrugated walls is considered more closely, allowing for parametric variations on the corrugation geometry. Finally, the heat transfer enhancement is inspected for a few different combinations of flow, thermal and geometric parameters, in terms of both the dimensionless bulk temperature and local Nusselt number along the heat transfer section.

ANALYSIS

We consider transient laminar forced convection within micro-channels formed by smooth or corrugated plates. Three regions along the channel are considered in the problem formulation, as described in Figure 1 below. First, an adiabatic region with smooth walls, followed by the heat transfer section with prescribed temperatures at the corrugated walls, and the third one, following the corrugated region, is again made of smooth adiabatic walls. The problem formulation adopts the same geometry and boundary conditions as presented by Wang & Chen [18]. The walls boundaries are then described by the following functions along the longitudinal coordinate:

$$fy_0^*(x^*)=\begin{cases} y_0^* & 0<x^*<L_1^*, \\ y_0^*+\alpha^*\ sen\left(\pi(x^*-L_1^*)\dfrac{12}{L_2^*}\right) & L_1^*<x^*<L_2^*, \\ y_0^* & L_2^*<x^*<L^*, \end{cases} \tag{1 a}$$

$$fy_1^*(x^*)=\begin{cases} y_1^* & 0<x^*<L_1^*. \\ y_1^*-\alpha^*\ sen\left(\pi(x^*-L_1^*)\dfrac{12}{L_2^*}\right) & L_1^*<x^*<L_2^*. \\ y_1^* & L_2^*<x^*<L^*. \end{cases} \tag{1 b}$$

The two-dimensional steady flow is assumed to be laminar and incompressible, with temperature independent thermophysical properties, while viscous dissipation and natural convection effects are neglected. Due to the possible low values of Peclet number, in light of the lower range of Reynolds numbers, axial diffusion along the fluid is not disregarded. Also, the flow is assumed to be fully developed at the first section entrance, but varies along the axial coordinate once the corrugated section is reached.

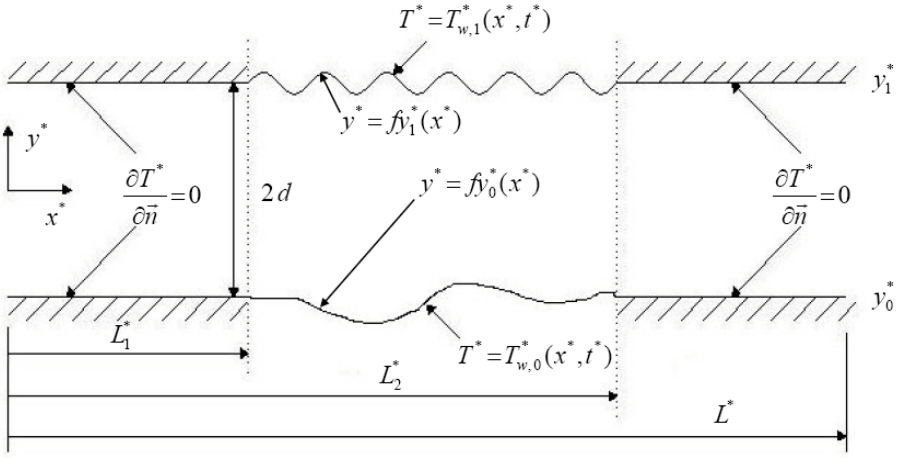

Fig. 1. Geometry and coordinates system for heat transfer in corrugated channel

In obtaining the velocity field along the flow, the full Navier-Stokes equations should be employed, yielding the variable velocity components and pressure field along the transversal and longitudinal directions, as recently demonstrated in [16-17], where the Generalized Integral Transform Technique (GITT) has been employed in the hybrid numerical-analytical solution of this laminar flow. However, for sufficiently low Reynolds numbers and smooth variations on the wall corrugations, an approximate solution has been previously proposed [7], essentially by accounting for the variable cross section within the local mass balance equation, but neglecting the momentum equations influence on the velocity components modification. These explicit solutions for the velocity components are particularly handy, especially in design and optimization tasks, and shall be here exploited to demonstrate the transient thermal problem solution. Thus, following this approach, the velocity components are analytically derived as:

$$u^*(x^*,y^*)=\frac{-(y_0^*-y_1^*)}{(fy_0^*(x^*)-fy_1^*(x^*))^3}\left[-y^{*2}+y^*(fy_0^*(x^*)+fy_1^*(x^*))-fy_0^*(x^*)\,fy_1^*(x^*)\right], \tag{2 a}$$

$$v^*(x^*,y^*)=\frac{-(y_0^*-y_1^*)}{(fy_0^*(x^*)-fy_1^*(x^*))^4}\Big[6(y-fy_0^*(x^*))(y-fy_1^*(x^*))\times \times\left(fy_1^{*}{}'(x^*)\;(y-fy_0^*(x^*))\;-\;fy_0^{*}{}'(x^*)\;(y-fy_1^*(x^*))\right)\Big]. \tag{2 b}$$

It can be noticed that according to the approximate solution in eqs.(2), at the entrance and exit of the corrugated section, as well as for a smooth heat transfer section, the flow becomes the classical parabolic fully developed velocity profile for parallel plates, given in the present coordinates system by:

$$u^*(y^*)=\frac{6}{(y_0^*-y_1^*)^2}\left[-y^{*2}+y^*(y_0^*+y_1^*)-y_0^*\,y_1^*\right], \tag{2 c}$$

while the transversal velocity component vanishes. Once the velocity field is available, the energy balance is given as:

$$\frac{\partial T^*(x^*,y^*,t^*)}{\partial t^*}+u^*(x^*,y^*)\frac{\partial T^*}{\partial x^*}+v^*(x^*,y^*)\frac{\partial T^*}{\partial y^*}=\alpha\left(\frac{\partial^2 T^*}{\partial x^{*2}}+\frac{\partial^2 T^*}{\partial y^{*2}}\right), \tag{3 a}$$

$$0<x^*<L^*,\, fy_0^*(x^*)<y^*<fy_1^*(x^*), t^*>0$$

$$T^*(x^*,y^*,0)=T_0^*(x^*,y^*),\quad T^*(0,y^*,t^*)=T_e^*(y^*,t^*),\quad \left.\frac{\partial T^*}{\partial x^*}\right|_{x^*=L^*}=0, \tag{3 b-d}$$

$$\text{for } 0<x^*<L_1^* \begin{cases}\left.\dfrac{\partial T^*}{\partial y^*}\right|_{y^*=fy_0^*(x^*)}=0\\ \left.\dfrac{\partial T^*}{\partial y^*}\right|_{y^*=fy_1^*(x^*)}=0\end{cases},\quad \text{for } L_1^*\le x^*\le L_2^* \begin{cases}T^*(x^*,y^*=fy_0^*(x^*),t^*)=T_{w,0}^*\\ T^*(x^*,y^*=fy_1^*(x^*),t^*)=T_{w,1}^*\end{cases} \tag{3 e-h}$$

$$\text{for } L_2^*<x^*<L^* \begin{cases}\left.\dfrac{\partial T^*}{\partial y^*}\right|_{y^*=fy_0^*(x^*)}=0\\ \left.\dfrac{\partial T^*}{\partial y^*}\right|_{y^*=fy_1^*(x^*)}=0.\end{cases} \tag{3 i, j}$$

The following dimensionless groups are defined:

$$\xi=\frac{\alpha}{u_m d}x^*=\frac{1}{Pe}\frac{x^*}{d},\quad y=\frac{y^*}{d},\quad u(\xi,y)=\frac{u^*(x^*,y^*)}{u_m},\quad v(\xi,y)=\frac{v^*(x^*,y^*)}{u_m},$$
$$t=\frac{\alpha}{d^2}t^*,\quad T_A(\xi,y,t)=\frac{T^*(x^*,y^*,t^*)-T_{w,0}^*}{\Delta T_c},\quad Pe=\frac{u_m d}{\alpha},\qquad d=\frac{y_1^*-y_0^*}{2}. \tag{4 a-g}$$

Then, the dimensionless form of the temperature problem is written as:

$$\frac{\partial T_A}{\partial t}+u(\xi,y)\frac{\partial T_A}{\partial \xi}+Pe\;v(\xi,y)\frac{\partial T_A}{\partial y}=\frac{1}{Pe^2}\frac{\partial^2 T_A}{\partial \xi^2}+\frac{\partial^2 T_A}{\partial y^2}, \tag{5 a}$$

$$0<\xi<L, fy_0(\xi)<y<fy_1(\xi), t>0.$$

$$T_A(\xi,y,0)=T_{A,0}(\xi,y),\quad T_A(0,y,t)=T_{A,e}(y,t),\quad \left.\frac{\partial T_A}{\partial \xi}\right|_{\xi=L}=0, \tag{5 b-d}$$

$$\text{for } 0<\xi<L_1 \quad \begin{cases} \left.\dfrac{\partial T_A}{\partial y}\right|_{y=fy_0(\xi)} = 0 \\ \left.\dfrac{\partial T_A}{\partial y}\right|_{y=fy_1(\xi)} = 0 \end{cases}, \quad \text{for } L_1 \le \xi \le L_2 \quad \begin{cases} T_A(\xi, y=fy_0(\xi), t) = 0, \\ T_A(\xi, y=fy_1(\xi), t) = T_{A,w,1}. \end{cases} \tag{5 e-h}$$

$$\text{for } L_2<\xi<L \quad \begin{cases} \left.\dfrac{\partial T_A}{\partial y}\right|_{y=fy_0(\xi)} = 0, \\ \left.\dfrac{\partial T_A}{\partial y}\right|_{y=fy_1(\xi)} = 0. \end{cases} \tag{5 i, j}$$

It can be observed from eqs. (5 g, h) that the formulation does not impose axial symmetry to the thermal problem, but if symmetry prevails, eq. (5 h) shall be an homogeneous one.

In light of the discontinuity on the boundary conditions at the junction of the three regions, it is adequate to propose a domain decomposition to handle the three mathematical problems separately, coupled at the cross sections between each pair of regions. The three problems formulation should therefore include the continuity conditions of temperature and heat flux at the fluid interfaces between the regions. Thus, the problem formulation for the first adiabatic region becomes:

$$\frac{\partial T_1}{\partial t} + u(\xi,y)\frac{\partial T_1}{\partial \xi} + Pe\ v(\xi,y)\frac{\partial T_1}{\partial y} = \frac{1}{Pe^2}\frac{\partial^2 T_1}{\partial \xi^2} + \frac{\partial^2 T_1}{\partial y^2}, \tag{6 a}$$

$$0 < \xi < L_1, fy_0(\xi) < y < fy_1(\xi), t > 0.$$

$$T_1(\xi, y, 0) = T_{A,0}(\xi, y), \tag{6 b}$$

$$T_1(0,y,t) = T_{A,e}(y,t), \quad \left.\frac{\partial T_1}{\partial \xi}\right|_{\xi=L_1} = \left.\frac{\partial T_{A,2}}{\partial \xi}\right|_{\xi=L_1}, \quad \left.\frac{\partial T_1}{\partial y}\right|_{y=fy_0(\xi)} = 0, \quad \left.\frac{\partial T_1}{\partial y}\right|_{y=fy_1(\xi)} = 0. \tag{6 c-f}$$

For the heat exchanging section, we have:

$$\frac{\partial T_{A,2}}{\partial t} + u(\xi,y)\frac{\partial T_{A,2}}{\partial \xi} + Pe\ v(\xi,y)\frac{\partial T_{A,2}}{\partial y} = \frac{1}{Pe^2}\frac{\partial^2 T_{A,2}}{\partial \xi^2} + \frac{\partial^2 T_{A,2}}{\partial y^2}, \tag{7 a}$$

$$L_1 < \xi < L_2, fy_0(\xi) < y < fy_1(\xi), t > 0.$$

$$T_{A,2}(\xi, y, 0) = T_{A,0}(\xi, y), \tag{7 b}$$

$$T_{A,2}(\xi = L_1, y, t) = T_1(\xi = L_1, y, t), \quad T_{A,2}(\xi = L_2, y, t) = T_3(\xi = L_2, y, t), \tag{7 c, d}$$

$$T_{A,2}(\xi, y = fy_0(\xi), t) = 0, \quad T_{A,2}(\xi, y = fy_1(\xi), t) = T_{A,w,1}. \tag{7 e, f}$$

and finally for the exiting section, also adiabatic:

$$\frac{\partial T_3}{\partial t} + u(\xi,y)\frac{\partial T_3}{\partial \xi} + Pe\ v(\xi,y)\frac{\partial T_3}{\partial y} = \frac{1}{Pe^2}\frac{\partial^2 T_3}{\partial \xi^2} + \frac{\partial^2 T_3}{\partial y^2}, \tag{8 a}$$

$$L_2 < \xi < L, fy_0(\xi) < y < fy_1(\xi), t > 0.$$

$$T_3(\xi, y, 0) = T_{A,0}(\xi, y), \tag{8 b}$$

$$\left.\frac{\partial T_3}{\partial \xi}\right|_{\xi=L_2} = \left.\frac{\partial T_{A,2}}{\partial \xi}\right|_{\xi=L_2}, \quad \left.\frac{\partial T_3}{\partial \xi}\right|_{\xi=L_1} = 0, \quad \left.\frac{\partial T_3}{\partial y}\right|_{y=fy_0(\xi)} = 0, \quad \left.\frac{\partial T_3}{\partial y}\right|_{y=fy_1(\xi)} = 0. \tag{8 c-f}$$

The temperature problem for the heated section remains non-homogeneous in eq.(7f). In order to homogenize the problem in the transversal direction *y*, a filtering solution, $\phi(\xi, y)$, is employed for the potential $T_{A,2}(\xi, y, t)$, in the form:

$$T_{A,2}(\xi,y,t)=T_2(\xi,y,t)+\phi(\xi,y)\,. \tag{9}$$

A simple and sufficiently general form for the filter $\phi(\xi,y)$ is obtained by satisfying the diffusion operator in the transversal direction, which yields:

$$\phi(\xi,y)=T_{A,w,1}\frac{fy_0(\xi)-y}{fy_0(\xi)-fy_1(\xi)}\,. \tag{10}$$

Then, the homogeneous problem for the corrugated section is given by:

$$\frac{\partial T_2}{\partial t}+u(\xi,y)\frac{\partial T_2}{\partial \xi}+Pe\;v(\xi,y)\frac{\partial T_2}{\partial y}=\frac{1}{Pe^2}\frac{\partial^2 T_2}{\partial \xi^2}+\frac{\partial^2 T_2}{\partial y^2}+g(\xi,y)\,, \tag{11 a}$$

$$L_1<\xi<L_2, fy_0(\xi)<y<fy_1(\xi), t>0\,.$$

$$T_2(\xi,y,t=0)=T_{A,0}(\xi,y)-\phi(\xi,y)\,, \tag{11 b}$$

$$T_2(\xi=L_1,y,t)=T_1(\xi=L_1,y,t)-\phi(\xi=L_1,y)\,,\quad T_2(\xi=L_2,y,t)=T_3(\xi=L_2,y,t)-\phi(\xi=L_2,y)\,, \tag{11 c, d}$$

$$T_2(\xi,y=fy_0(\xi),t)=0\,,\quad T_2(\xi,y=fy_1(\xi),t)=0\,. \tag{11 e, f}$$

where

$$g(\xi,y)=\frac{1}{Pe^2}\frac{\partial^2\phi}{\partial\xi^2}-Pe\;v(\xi,y)\frac{\partial\phi}{\partial\xi}-u(\xi,y)\frac{\partial\phi}{\partial y}\,. \tag{11 g}$$

Next, the decomposed domain is described with three different coordinates systems, which match at the two interfaces, as shown in Figure 2 below. The normalized longitudinal coordinates are then computed in terms of the original dimensionless coordinate as:

$$x_1=\frac{1}{L_1}\xi\,,\quad x_2=\frac{1}{(L_2-L_1)}(L_2-\xi)\,,\quad x_3=\frac{1}{(L-L_2)}(\xi-L_2)\,. \tag{12}$$

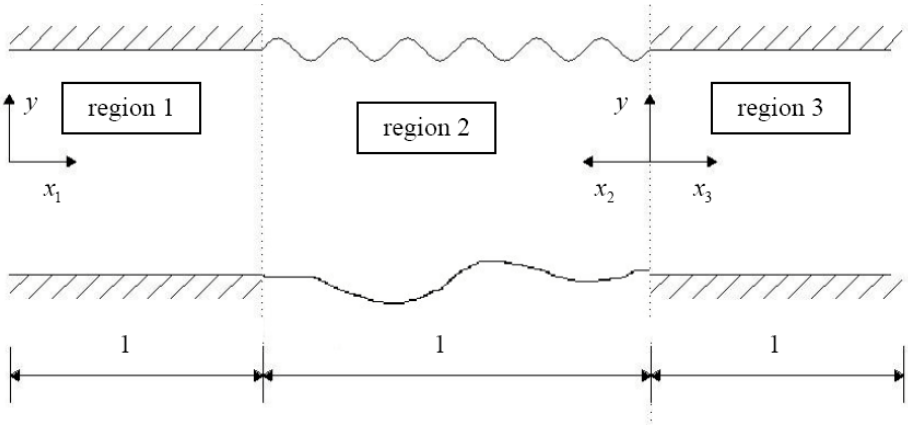

Fig. 2. Coordinates systems for the decomposed domain

Thus, in terms of the redefined coordinates systems the dimensionless problem formulation is given, for each of the three regions, as:

$$\frac{\partial T_1}{\partial t}+u(x_1,y)\frac{\partial T_1}{\partial x_1}\frac{1}{L_1}+Pe\;v(x_1,y)\frac{\partial T_1}{\partial y}=\frac{1}{Pe^2}\frac{1}{L_1^2}\frac{\partial^2 T_1}{\partial x_1^2}+\frac{\partial^2 T_1}{\partial y^2}\,,\ 0<x_1<1, y_0<y<y_1, t>0\,. \tag{13 a}$$

$$T_1(x_1,y,t=0)=T_{1,0}(x_1,y)\,, \tag{13 b}$$

$$T_1(x_1=0,y,t)=T_{A,e}(y,t)\,,\quad \left.\frac{\partial T_1}{\partial x_1}\right|_{x_1=1}=-\left.\frac{\partial T_2}{\partial x_2}\right|_{x_2=1}\frac{L_1}{L_2-L_1}\,, \tag{13 c, d}$$

$$\left.\frac{\partial T_1}{\partial y}\right|_{y=y_0}=0\,,\quad \left.\frac{\partial T_1}{\partial y}\right|_{y=y_1}=0\,, \tag{13 e, f}$$

$$\frac{\partial T_2}{\partial t}+u(x_2,y)\frac{\partial T_2}{\partial x_2}\left(\frac{-1}{(L_2-L_1)}\right)+Pe\ v(x_2,y)\frac{\partial T_2}{\partial y}=\frac{1}{Pe^2}\frac{1}{(L_2-L_1)^2}\frac{\partial^2 T_2}{\partial x_2^2}+ \\ +\frac{\partial^2 T_2}{\partial y^2}+g(x_1,y)\quad ,0<x_2<1, fy_0(x_2)<y<fy_1(x_2), t>0, \tag{14 a}$$

$$T_2(x_2,y,t=0)=T_{2,0}(x_2,y)-\phi(x_2,y), \tag{14 b}$$

$$T_2(x_2=0,y,t)=T_3(x_3=0,y,t)-\phi(x_2=0,y), \quad T_2(x_2=1,y,t)=T_1(x_1=1,y,t)-\phi(x_2=1,y), \tag{14 c, d}$$

$$T_2(x_2,y=fy_0(x_2),t)=0, \quad T_2(x_2,y=fy_1(x_2),t)=0, \tag{14 e, f}$$

$$\phi(x_2,y)=T_{A,w,1}\frac{fy_0(x_2)-y}{fy_0(x_2)-fy_1(x_2)}, g(x_2,y)=\frac{1}{Pe^2(L_2-L_1)^2}\frac{\partial^2\phi}{\partial x_2^2}-Pe\ v(x_2,y)\frac{\partial\phi}{\partial y}+u(x_2,y)\frac{\partial\phi}{\partial x_2}\frac{1}{L_2-L_1}, \tag{14g,h}$$

$$\frac{\partial T_3}{\partial t}+u(x_3,y)\frac{\partial T_3}{\partial x_3}\frac{1}{(L-L_2)}+Pe\ v(x_3,y)\frac{\partial T_3}{\partial y}=\frac{1}{Pe^2}\frac{1}{(L-L_2)^2}\frac{\partial^2 T_3}{\partial x_3^2}+\frac{\partial^2 T_3}{\partial y^2}, \\ 0<x_3<1, y_0<y<y_1, t>0. \tag{15 a}$$

$$T_3(x_3,y,t=0)=T_{3,0}(x_3,y), \tag{15 b}$$

$$\left.\frac{\partial T_3}{\partial x_3}\right|_{x_3=0}=-\left.\frac{\partial T_2}{\partial x_2}\right|_{x_2=0}\frac{L-L_2}{L_2-L_1}, \quad \left.\frac{\partial T_3}{\partial x_3}\right|_{x_3=1}=0, \tag{15 c, d}$$

$$\left.\frac{\partial T_3}{\partial y}\right|_{y=y_0}=0, \quad \left.\frac{\partial T_3}{\partial y}\right|_{y=y_1}=0. \tag{15 e, f}$$

One may observe that after the coordinates systems redefinition, the problems are coupled only at the interfaces and all the domains limits are the same, and therefore the dependent variables may be algebraically interpreted as applied to one single domain in the longitudinal coordinate (0<x<1).

Following the formalism in the GITT [8–10], the auxiliary problems are now defined to construct the eigenfunction expansions in each region. For regions 1 and 3 we adopt the same eigenvalue problem, with second kind boundary conditions, given by:

$$\frac{d^2\psi_i}{dy^2}+\mu_i^2\,\psi_i(y)=0, \quad y_0<y<y_1,\ y_0<y<y_1, \tag{16 a}$$

$$\left.\frac{d\psi_i}{dy}\right|_{y=y_0}=0, \quad \left.\frac{d\psi_i}{dy}\right|_{y=y_1}=0. \tag{16 b, c}$$

whose solution in terms of eigenfunctions, norms and eigenvalues is readily found as

$$\psi_i(y)=\begin{cases}1, i=0,\\ \cos(\mu_i(y-y_0)), i=1,2,3...,\end{cases} \quad N\psi_i=\int_{y_0}^{y_1}\psi_i^2(y)\,dy=\begin{cases}y_1-y_0, i=0,\\ \dfrac{y_1-y_0}{2}, i=1,2,3...,\end{cases} \\ \mu_i=\begin{cases}0, i=0\\ \dfrac{i\pi}{y_1-y_0}, i=1,2,3...\end{cases} \tag{16 d-f}$$

For region 2, the auxiliary problem has to account for the irregular walls, which is incorporated into the eigenfunctions and eigenvalues via the functions of *x* that describe the transversal domains, as shown below:

$$\frac{\partial^2\Gamma_m}{\partial y^2}+\beta_m^2(x)\,\Gamma_m(x,y)=0, \quad fy_0(x)<y<fy_1(x),\ fy_0(x)<y<fy_1(x), \tag{17 a}$$

$$\Gamma_m(y=fy_0(x))=0, \quad \Gamma_m(y=fy_1(x))=0. \tag{17 b, c}$$

Thus, the *x*-dependent eigenfunctions, norms and eigenvalues are given by:

$$\Gamma_m(x,y)=\mathrm{sen}\left(\beta_m(x)\,(y-fy_0(x))\right),$$

$$N\Gamma_m(x)=\int_{fy_0(x)}^{fy_1(x)}\Gamma_m^2(x,y)\,dy=\frac{fy_1(x)-fy_0(x)}{2},\quad \beta_m(x)=\frac{m\pi}{fy_1(x)-fy_0(x)},\quad m=1,2,3\ldots. \tag{17 d-f}$$

Once the eigenvalue problems have been defined and solved, the integral transform pairs (transform-inverse) are constructed as:

$$\overline{T}_{1,i}(x,t)=\int_{y_0}^{y_1}T_1(x,y,t)\,\psi_i(y)\,dy,\quad T_1(x,y,t)=\sum_{i=0}^{\infty}\frac{1}{N\psi_i}\overline{T}_{1,i}(x,t)\,\psi_i(y)\ \text{transform}, \tag{18 a, b}$$

$$\overline{T}_{2,m}(x,t)=\int_{fy_0(x)}^{fy_1(x)}T_2(x,y,t)\,\Gamma_m(x,y)\,dy,\quad T_2(x,y,t)=\sum_{m=1}^{\infty}\frac{1}{N\Gamma_m(x)}\overline{T}_{2,m}(x,t)\,\Gamma_m(x,y)\ \text{transform}, \tag{19 a, b}$$

$$\overline{T}_{3,i}(x,t)=\int_{y_0}^{y_1}T_3(x,y,t)\,\psi_i(y)\,dy,\quad T_3(x,y,t)=\sum_{i=0}^{\infty}\frac{1}{N\psi_i}T_{3,i}(x,t)\,\psi_i(y)\ \text{transform}. \tag{20 a, b}$$

One may start with the integral transformation of eqs.(13) for region 1, operating with $\int_{y_0}^{y_1}\bullet\,\psi_i(y)\,dy$, and after substitution of the inverse formula (18b) and some manipulation, the transformed system becomes:

$$\frac{\partial\overline{T}_{1,i}}{\partial t}+\frac{1}{L_1}\sum_{j=0}^{\infty}A_{ij}\frac{\partial\overline{T}_{1,j}}{\partial x}=\frac{1}{Pe^2\,L_1^2}\frac{\partial^2\overline{T}_{1,i}}{\partial x^2}-\mu_i^2\,\overline{T}_{1,i}(x,t),\ 0<x<1, t>0, \tag{21 a}$$

$$\overline{T}_{1,i}(x,t=0)=\overline{T}_{1,0,i}(x), \tag{21 b}$$

$$\overline{T}_{1,i}(x=0,t)=\overline{T}_{e,i}(t),\quad \left.\frac{\partial\overline{T}_{1,i}}{\partial x}\right|_{x=1}=-\frac{L_1}{L_2-L_1}\sum_{n=1}^{\infty}\frac{1}{N\Gamma_n(x=1)}B_{in}(x=1)\left.\frac{\partial\overline{T}_{2,n}}{\partial x}\right|_{x=1}. \tag{21 c, d}$$

Similarly, eqs.(14) are operated on with $\int_{fy_0(x)}^{fy_1(x)}\bullet\,\Gamma_m(x,y)\,dy$ to yield the transformed version for the temperature problem in region 2:

$$\begin{aligned}\frac{\partial\overline{T}_{2,m}}{\partial t}=&\frac{1}{Pe^2\,(L_2-L_1)^2}\frac{\partial^2\overline{T}_{2,m}}{\partial x^2}+\\&+\sum_{n=1}^{\infty}\frac{\partial\overline{T}_{2,n}}{\partial x}\left[\frac{1}{Pe^2\,(L_2-L_1)^2}\left(2\frac{d}{dx}\left(\frac{1}{N\Gamma_n(x)}\right)N\Gamma_n(x)\delta_{mn}+\frac{2}{N\Gamma_n(x)}F_{mn}(x)\right)+\right.\\&\left.+\frac{1}{L_2-L_1}\left(\frac{1}{N\Gamma_n(x)}D_{mn}(x)\right)\right]+\sum_{n=1}^{\infty}\overline{T}_{2,n}(x,t)\left[\frac{1}{Pe^2\,(L_2-L_1)^2}\times\right.\\&\times\left(\frac{d^2}{dx^2}\left(\frac{1}{N\Gamma_n(x)}\right)N\Gamma_n(x)\delta_{mn}+2\frac{d}{dx}\left(\frac{1}{N\Gamma_n(x)}\right)F_{mn}(x)+\frac{1}{N\Gamma_n(x)}G_{mn}(x)\right)+\\&+\frac{1}{L_2-L_1}\left(\frac{1}{N\Gamma_n(x)}C_{mn}(x)+\frac{d}{dx}\left(\frac{1}{N\Gamma_n(x)}\right)D_{mn}(x)\right)-\\&\left.-Pe\left(\frac{1}{N\Gamma_n(x)}E_{mn}(x)\right)-\beta_m^2(x)\,\delta_{mn}\right]+\overline{g}_m(x),0<x<1,\ t>0,\end{aligned} \tag{22 a}$$

$$\overline{T}_{2,m}(x,t=0)=\overline{T}_{2,0,m}(x)-\overline{\phi}_m(x), \tag{22 b}$$

$$\overline{T}_{2,m}(x=0,t)=\sum_{j=0}^{\infty}\left(\frac{1}{N\psi_j}B_{mj}(x=0)\,\overline{T}_{3,j}(x=0,t)\right)-\overline{\phi}_m(x=0), \tag{22 c}$$

$$\overline{T}_{2,m}(x=1,t)=\sum_{j=0}^{\infty}\left(\frac{1}{N\psi_j}B_{mj}(x=1)\,\overline{T}_{1,j}(x=1,t)\right)-\overline{\phi}_m(x=1). \tag{22 d}$$

And finally, for region 3, eqs.(15) are operated on with $\int_{y_0}^{y_1} \bullet \psi_i(y)\,dy$, to furnish:

$$\frac{\partial \overline{T}_{3,i}}{\partial t} + \frac{1}{L-L_2}\sum_{j=0}^{\infty} A_{ij}\frac{\partial \overline{T}_{3,j}}{\partial x} = \frac{1}{Pe^2\,(L-L_2)^2}\frac{\partial^2 \overline{T}_{3,i}}{\partial x^2} - \mu_i^2\,\overline{T}_{3,i}(x,t)\,,\ 0<x<1, t>0\,, \tag{23 a}$$

$$\overline{T}_{3,i}(x,t=0) = \overline{T}_{3,0,i}(x)\,, \tag{23 b}$$

$$\left.\frac{\partial \overline{T}_{3,i}}{\partial x}\right|_{x=0} = -\frac{L-L_2}{L_2-L_1}\sum_{n=1}^{\infty}\frac{1}{N\Gamma_m(x=0)}B_{in}(x=0)\left.\frac{\partial \overline{T}_{2,n}}{\partial x}\right|_{x=0}\,,\quad \left.\frac{\partial \overline{T}_{3,i}}{\partial x}\right|_{x=1} = 0\,. \tag{23 c, d}$$

The coefficients that appear on the transformed system eqs.(21)–(23) are analytically obtained from the following integrations:

$$A_{ij} = \frac{1}{N\psi_j}\int_{y_0}^{y_1} u(y)\psi_i(y)\psi_j(y)\,dy\ ,\quad B_{ni}(x) = \int_{y_0}^{y_1}\psi_i(y)\Gamma_n(x,y)\,dy\,, \tag{24 a, b}$$

$$C_{mn}(x) = \int_{fy_0(x)}^{fy_1(x)} u(x,y)\Gamma_m(x,y)\frac{\partial \Gamma_n}{\partial x}dy\,,\quad D_{mn}(x) = \int_{fy_0(x)}^{fy_1(x)} u(x,y)\Gamma_m(x,y)\Gamma_n(x,y)\,dy\,, \tag{24 c, d}$$

$$E_{mn}(x) = \int_{fy_0(x)}^{fy_1(x)} v(x,y)\Gamma_m(x,y)\frac{\partial \Gamma_n}{\partial y}dy\,,\quad F_{mn}(x) = \int_{fy_0(x)}^{fy_1(x)} \Gamma_m(x,y)\frac{\partial \Gamma_n}{\partial x}dy\,, \tag{24 e, f}$$

$$G_{mn}(x) = \int_{fy_0(x)}^{fy_1(x)} \Gamma_m(x,y)\frac{\partial^2 \Gamma_n}{\partial x^2}dy\,,\quad \overline{g}_m(x) = \int_{fy_0(x)}^{fy_1(x)} g(x,y)\Gamma_m(x,y)\,dy\,, \tag{24 g, h}$$

$$\overline{\phi}_m(x) = \int_{fy_0(x)}^{fy_1(x)} \phi(x,y)\Gamma_m(x,y)\,dy\,. \tag{24 i}$$

Eqs. (21)–(23) form an infinite system of partial differential equations having as independent variables the unified dimensionless longitudinal coordinate, *x*, and dimensionless time, *t*, and as dependent variables the transformed temperatures in each region. For computational purposes, the system is truncated to a finite order, truncating the eigenfunction expansions for each field in a sufficiently large number of terms for each region (N_1, N_2 and N_3). Due to the x-variable nature of the system coefficients, eqs.(24), the PDE system has to be numerically solved, for instance employing the Method of Lines with local error control as implemented on the function NDSolve of the *Mathematica* 5.2 symbolic-numerical computation platform [11].

For the thermal problem, results are reported in terms of the bulk temperature and the local Nusselt numbers at the two channel walls (yielding the same results for the symmetric situation), as defined below:

$$T_m(\xi,t) = \frac{\int_{fy_0(\xi)}^{fy_1(\xi)} u(\xi,y)\,T_A(\xi,y,t)\,dy}{\int_{fy_0(\xi)}^{fy_1(\xi)} u(\xi,y)\,dy}\,, \tag{25 a}$$

$$Nu_1(\xi,t) = \frac{-4}{T_m(\xi,t)}\left(\nabla T_A\cdot\mathbf{n}_{y_1}\right),\quad Nu_0(\xi,t) = \frac{4}{T_m(\xi,t)}\left(\nabla T_A\cdot\mathbf{n}_{y_0}\right). \tag{25 b, c}$$

RESULTS AND DISCUSSION

The constructed computer code was first verified against the thermal problem results for transient convection within smooth parallel-plates channels [14] with one single region, i.e., only the heat transfer section. A thorough convergence analysis was then undertaken on the bulk and local temperature results so as to provide confidence on the numerical results to be now reported. As a consolidation of such analysis, the adoption of truncation orders of $N_1 = 4$, $N_2 = 8$ and $N_3 = 4$ were sufficient to provide three to four significant digits in the temperature field results, in a fairly wide

range of the dimensionless longitudinal coordinate and for the values of Peclet number Pe =1, 10 and 30, to be reported below. It was also concluded that the order of the expansions is required to gradually increase as Pe increases.

It was found of interest to also validate the present analysis for smooth parallel plates against a previously reported analytical solution [19] that accounts for the upstream adiabatic region, under steady laminar forced convection for low Peclet numbers. Figure 3 thus presents such comparison in terms of the dimensionless bulk temperature, where only the results along the heat transfer section are presented. Different values of a modified Peclet number are employed, named Pe_T , according to the definition in [19]. A fairly good adherence between the two independent solutions can be observed providing further validation to the proposed hybrid methodology. Also, one may already observe the marked influence of the axial diffusion along the fluid on the temperature behavior within the actual heat trasnfer section.

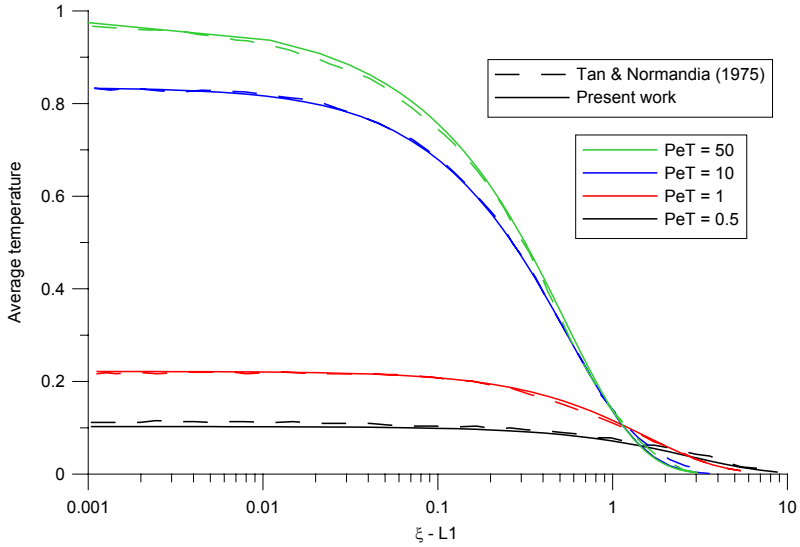

Fig. 3. Comparison of dimensionless bulk temperatures from present GITT solution and from analytical steady-state solution in [19] for a smooth parallel-plates channel with an upstream adiabatic region and low Peclet number

Figure 4 now illustrates the influence of the axial heat diffusion within the fluid more closely, showing the steady-state dimensionless bulk temperatures along the channel for Pe = 1, 10, and 30, and especially across the interface between the upstream adiabatic region and the heat transfer section. The pre-cooling (or heating) effect provided by the presence of the upstream region is quite noticeable for the lower values of Peclet number, which is quite relevant along the transient state as well, as also shown in Figure 5 for Pe = 30. As a result, a heat transfer enhancement effect is in fact observed, resulting in higher values of the Nusselt number in this region for decreasing Peclet number. As can be deduced, significant errors may result if experimental results are employed to estimate average Nusselt numbers that assume the bulk temperature at the heat transfer section inlet as the uniform temperature at the upstream region inlet.

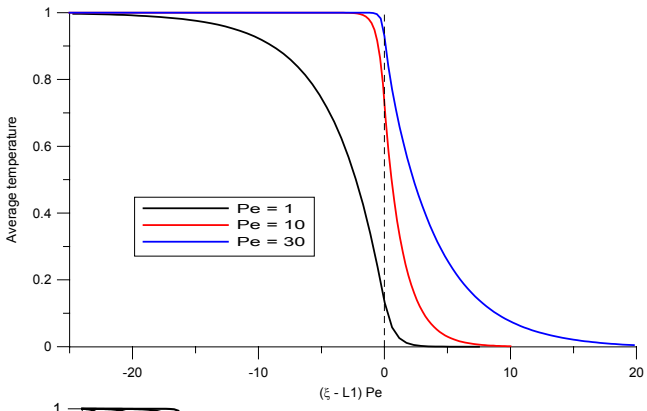

Fig. 4. Comparison of dimensionless bulk temperatures in smooth parallel-plates channel along both the upstream adiabatic region and heat transfer section at steady-state for different values of Peclet number (dashed line is the interface between the two regions)

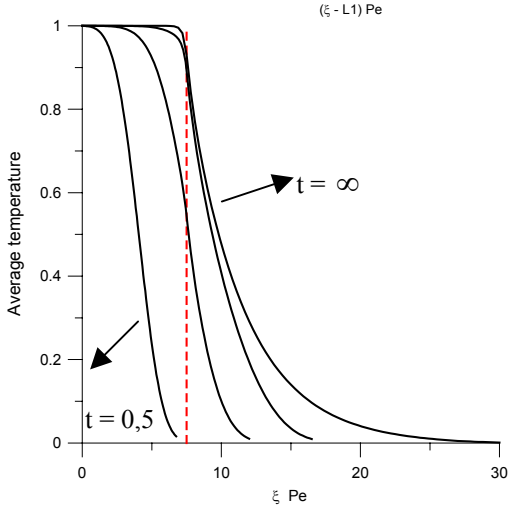

Fig. 5. Transient behavior of the dimensionless bulk temperature in smooth parallel-plates channel along both the upstream adiabatic region and the heat transfer section for Pe = 30 and t = 0.5, 1.0, 1.5 and steady-state (dashed line is the interface between the two regions)

The next step in the present analysis is the verification of the adequacy of the approximate velocity field, eqs. (2), in describing the flow behavior within the corrugated channel. As previously mentioned, the simplified approach is expected to provide reasonable results for lower values of the Reynolds number and for smoother corrugations. Thus, numerical results for the full Navier-Stokes formulation were employed in the verification of the present approximate analytical solutions, as obtained from the GITT hybrid numerical-analytical solution available in [16, 17]. For instance, Figure 6.a presents the longitudinal velocity component at different axial positions along the corrugated section, for the chosen values of Re = 10 and α = 0.1, while Fig. 6b presents the velocity component for a less smooth corrugation, with α = 0.2.

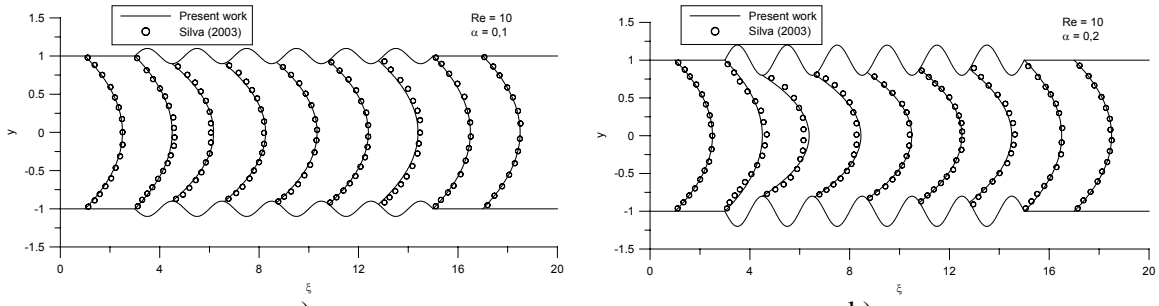

a) b)

Fig. 6. Comparison of longitudinal velocity component for corrugated channel between present approximate results and GITT solution of [16, 17], for: a) Re = 10, α = 0.1 and b) Re = 10, α = 0.2

It can be noticed that the increase in the wall corrugation amplitude leads to a less accurate velocity component as obtained from the approximate relations of eqs.(2), especially in regions closer to the inlet of the corrugated region. Also, increasing the Reynolds number leads to some loss of accuracy in the simplified solution, but one can see from Figure 7 below that the results are still reasonably accurate for the case of Re = 100 and α = 0.1, and apparently the increase in corrugation

amplitude of Fig. 6b was more significant in deviating the approximate solution from the converged GITT results for the full Navier-Stokes formulation than the increase in Reynolds number of Fig. 7. The comparisons of the longitudinal velocity component are emphasized since the related convective term is the most important one in the heat transfer problem to be addressed.

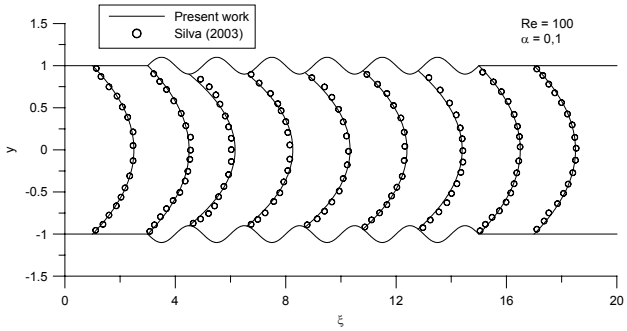

Fig. 7. Comparison of longitudinal velocity component for corrugated channel between present approximate results and GITT solution of [16,17], for Re = 100 and α = 0.1

Figure 8 illustrates the transient behavior of the bulk temperature for Pe = 10, where the dashed red line denotes the interface between the adiabatic region 1 and the corrugated section, region 2. Clearly, we may see that due to the low Reynolds number value (and consequently low Peclet number), the axial diffusion along the fluid promotes a sensible effect on the bulk temperature evolution within the access region (region 1) along the transient period. The steady-state results are however closer to the situation of an unheated inlet section, which would be obtained by the model that neglects axial diffusion of heat within the fluid. Therefore, for micro-channel applications that involve low Peclet numbers, the behavior of the thermal wave front can be markedly affected by the presence of an adiabatic inlet section. It can also be observed that the bulk temperature behavior presents a typical fluctuating shape due to the presence of the wall corrugations.

Next, Figure 9 illustrates the effect of the Peclet number on the bulk temperatures for the steady-state situation, by taking the two values Pe = 10 and 30. Similarly to the smooth channel situation, one may clearly observe the more significant pre-heating effect in region 1 due to the lower value of Pe, but also the more pronounced effects on the bulk temperature fluctuations due to the wall corrugations in the case of a smaller axial diffusion of heat, when the transversal effects start playing a major role.

For the heat transfer enhancement analysis it is of interest to evaluate the behavior of the Nusselt number under different corrugation conditions. Figure 10, for instance, illustrates the local Nusselt number results for Pe = 10 and α = 0.1 and 0.2. The smooth parallel plates case is also plotted for reference purposes, as the solid black line. One may see that even with the lower corrugation amplitude value some noticeable heat transfer enhancement is already evident, and marked increases in the local heat transfer coefficient are achieved for the higher corrugation amplitude value for this value of Pe.

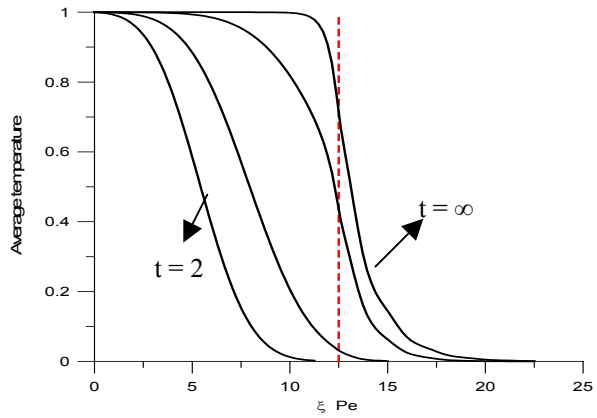

Fig. 8. Transient behavior of bulk temperature on regions 1 and 2 for Pe = 10, α = 0.1, and t = 2, 3, 5, steady-state

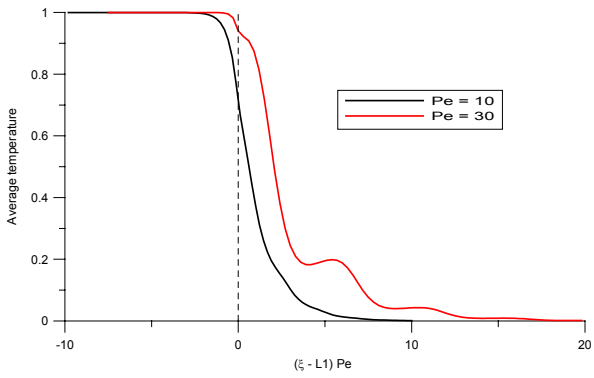

Fig. 9. Influence of Peclet number on the bulk temperature behavior along regions 1 and 2 in steady-state, for Pe = 10 and 30, α = 0.1

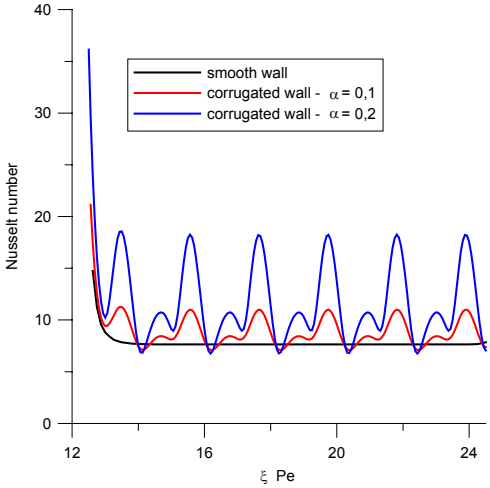

Fig. 10. Local Nusselt numbers at steady-state for smooth and corrugated channels with Pe = 10 and α = 0 (parallel-plates), 0.1 and 0.2

CONCLUSION

Laminar forced convection within micro-channels with smooth and corrugated walls was analyzed and discussed to investigate possible heat transfer enhancement effects. The physical modeling for the thermal problem includes discontinuities in the boundary conditions at the channel walls, considering the interfaces between entrance and exit adiabatic regions and an intermediate heat transfer section. The thermal problem was then solved with the Generalized Integral Transform Technique (GITT) applied in partial transformation mode and with a transient formulation. The presented results exploited the average temperature field within the micro-channel and the local Nusselt number within the heat transfer section of the channel. The axial diffusion effect along the fluid was first examined for a smooth parallel-plates channel, in light of the lower values of Peclet number achievable in such applications due to the low values of Reynolds number. The importance of accounting for an upstream adiabatic region was discussed, illustrating the resulting marked changes on the temperature distribution behavior within the actual heat transfer section. Then, for the corrugated heat transfer section case, the velocity field was obtained by making use of an approximate solution methodology, shown to be appropriate for small scale corrugations and low Reynolds numbers. From such results, one may notice the combined influence on the enhancement in local Nusselt number values along the heat transfer section due to both the low values of Peclet number and the presence of corrugated walls. The analysis may now proceed towards the more accurate solution of the flow problem employing the GITT itself, as previously accomplished in [16, 17], and also to the utilization of optimization schemes towards the identification of wall profiles for optimally enhanced heat transfer.

Acknowledgements

The authors would like to acknowledge the partial financial support provided by CNPq, and Petrobras S. A., along the developments here reported.

References

1. Webb R. L. & Kim N. H., *Principles of Enhanced Heat Transfer*, 2nd edition, Taylor & Francis Group, New York, NY, EUA, 2005.
2. Yener Y., Kakaç S., Avelino M., Okutucu T. Single-phase forced convection in micro-channels – a state-of-the-art review // *NATO ASI Series, Microscale Heat Transfer*, S. Kakaç *et al*. (eds.), 2005. Pp. 1–24.
3. Steinke M. E., Kandlikar S. G. Single-phase heat transfer enhancement techniques in micro-channel and mini-channel flows // *Proc. of the Intern. Conf. on Micro-channels and Mini-channels – ASME*, Rochester, NY, June, 2004.
4. Vasudevaiah M., Balamurugan K. Heat transfer of rarefied gases in a corrugated micro-channel, *Intern. J. Thermal Sciences. 2001*. Vol. 40. Pp. 454–468.

5. Chen C. K., Cho C. C. Electrokinetically-driven flow mixing in micro-channels with wavy surface // *J. of Colloid and Interface Science*, 2007. Vol. 312. Pp. 470–480.
6. Castellões F. V. *Transient Convection in Micro-channels via Integral Transforms*, M.Sc. Thesis, COPPE / UFRJ, Brazil (in Portuguese), 2004.
7. Ozisik M. N., Trepp C., Egolf H. Laminar forced convection in converging or diverging planar symmetric ducts // *Intern. J. of Heat and Mass Transfer*, 1982. Vol. 25 (10). Pp. 1477–1480.
8. Cotta R. M. *Integral Transforms in Computational Heat and Fluid Flow*, , Boca Raton, Florida, CRC Press, USA, 1993.
9. Cotta R. M., Ed. *The Integral Transforms Method in Thermal and Fluids Sciences and Engineering*, New York: Begell House USA, 1998.
10. Cotta R. M. and Mikhailov M. D. Hybrid Methods and Symbolic Computations // *Handbook of Numerical Heat Transfer*, 2nd edition, Chapter 16 / Eds. W.J. Minkowycz, E.M. Sparrow, J.Y. Murthy, John Wiley, New York, 2006. Pp. 493–522.
11. Wolfram S. *The Mathematica Book*, version 5.2, Cambridge-Wolfram Media, 2005.
12. Cotta R.M., Gerk J.E.V. Mixed finite-difference / integral transform approach for parabolic-hyperbolic problems in transient forced convection // *Numerical Heat Transfer, Part B*, 1994. Vol. 25, Pp. 433–448.
13. Cotta R.M., S. Kakaç, M.D. Mikhailov, F.V. Castellões, and C.R. Cardoso Transient Flow and Thermal Analysis in Microfluidics // *NATO ASI – Advanced Study Institute on Micro-Scale Heat Transfer: Fundamentals and Applications in Biological and Microelectromechanical systems,* Çesme, Turkey, July 18-30, 2004; also, *NATO ASI Series, Microscale Heat Transfer*, S. Kakaç et al. (eds.), 2005. Pp. 175–196.
14. Castellões F.V. and Cotta R.M. Analysis of transient and periodic convection in micro-channels via Integral Transforms // *Proc. of the 4th ICCHMT*, Paris, France, May, 2005; also *Progress in Computational Fluid Dynamics*, 2006. Vol. 6 (6), Pp. 321–326.
15. Castellões F. V., C. R. Cardoso, P. Couto, and R. M. Cotta, ransient Analysis of Slip Flow and Heat Transfer in Microchannels // *Proc. of 10th Brazilian Congress of Thermal Sciences and Engineering, ENCIT 2004*, Rio de Janeiro, RJ, November-December, 2004; also, *Heat Transfer Eng.*, 2007. Vol. 28, no.6, Pp. 549–558.
16. Silva R.L.; Quaresma J.N.N.; Santos C.A.C. Hybrid Solution for Flow Development in Irregular Ducts // *Proc. of the 10th Brazilian Congress of Thermal Sciences and Engineering, 2004 - ENCIT-2004*, Rio de Janeiro, 2004.
17. Silva R.L.; Santos C.A.C.; Quaresma J.N.N.; Cotta R.M., Hybrid Solution for Developing Laminar Flow in Wavy-Wall Channels via Integral Transforms // *Proc. of the 2007 ASME International Mechanical Engineering Congress & Exposition - IMECE2007*, Seattle, 2007.
18. Wang C. C., Chen C.K. Forced convection in a wavy-wall channel // *Intern. J. of Heat and Mass Transfer*, 2002. Vol. 45, Pp. 2587–2595.
19. Tan C. W., Normandia M. J. Low Peclet number diffusion in narrow rectangular channels // *Letters in Heat and Mass Transfer*, 1975. Vol. 2, Pp. 259–266.